ELSEVIER

Journal of Computational and Applied Mathematics 128 (2001) 235–260

JOURNAL OF COMPUTATIONAL AND APPLIED MATHEMATICS

www.elsevier.nl/locate/cam

The p and hp finite element method for problems on thin domains

Manil Suri [*, 1]

Department of Mathematics and Statistics, University of Maryland Baltimore County, Baltimore, MD 21250, USA

Received 27 August 1999; received in revised form 7 October 1999

Abstract

The p and hp versions of the finite element method allow the user to change the polynomial degree to increase accuracy. We survey these methods and show how this flexibility can be exploited to counter four difficulties that occur in the approximation of problems over *thin* domains, such as plates, beams and shells. These difficulties are: (1) control of modeling error, (2) approximation of corner singularities, (3) resolution of boundary layers, and (4) control of locking. Our guidelines enable the efficient resolution of these difficulties when a p/hp code is available. © 2001 Elsevier Science B.V. All rights reserved.

MSC: 65N30

Keywords: p version; hp version; Boundary layers; Hierarchical modeling; Plates; Singularities; Locking

1. Introduction

The classical 1956 reference [42] contains one of the first published systematic description of finite elements. The elements described in this paper (such as the Turner rectangle, the Timoshenko beam element and the linear triangle (first proposed by Courant in 1943)) use linear (or bilinear) piecewise polynomials to approximate the solution, and depend on mesh refinement for increased accuracy. This philosophy, of using low-order polynomials over successively finer meshes, has been the predominant one considered by researchers for many years, and was the one under which the development of the finite element method proceeded (with much success) through the 1970s.

* Fax: 1-410-455-1066.

E-mail address: suri@math.umbc.edu (M. Suri).

[1] Supported in part by the Air Force Office of Scientific Research. Air Force Systems Command, USAF, under grant F49620-98-1-0161 and the National Science Foundation under grant DMS-9706594.

PII: S0377-0427(00)00514-8

Experiments by Szabo and his group conducted in the mid-1970s [41] indicated that an alternative strategy might hold great promise as well. Their idea was to keep the mesh fixed, but increase the polynomial degree for accuracy. They called this the p version, to distinguish it from the classical method, which was labelled the h version. Computations on the elasticity problem indicated that this new philosophy was always competitive with, and often out-performed, the traditional h version. The first theoretical paper on the p version was published by Babuška et al. in 1981 [11], and showed, among other results, that the convergence rate was *double* that the h version for domains with corners, and *exponential* for smooth solutions.

The collaboration between Babuška and Szabo also led to the development of the so-called hp version, which combines both strategies. It was shown that with proper mesh selection/refinement coupled with increase of polynomial degrees, an exponential convergence rate could be achieved even for unsmooth solutions, i.e. in the presence of corner singularities. The first mathematical paper on the hp version was by Babuška and Dorr, and appeared in 1981 [2].

Since the advent of these first results, the p and hp versions have, over the past two decades, come into their own as viable complements to the h version. Various commercial codes, such as STRESS CHECK, POLYFEM, PHLEX, APPLIED STRUCTURE, MSC-NASTRAN (among others) have either been developed or modified to include p/hp capability. While no single strategy (such as h, p or hp refinement) can be expected to be optimal for all problems, having both h and p capability allows a level of flexibility that can often be exploited to significantly increase accuracy and efficiency. In particular, the high rates of convergence afforded by p/hp techniques when corner (r^α) singularities are present in the solution puts these methods ahead of traditional h-refinement for some important classes of problems.

In this paper, we bring out some of these advantages of p/hp methods. Rather than give a general survey of such methods (for which the reader is referred, e.g., to [9], and to the books [40,31]), we list some important properties in Section 2, and then concentrate mainly on one class of problems — that of linear elasticity posed on *thin* domains such as beams, plates and shells. This class of problems is one that comes up very frequently in engineering structural analysis. In Sections 3–6, we discuss four areas where p/hp capability leads to advantages in approximation: (1) control of *modeling error*, (2) good approximation of *singularities* occurring at the corners of the domain, (3) accurate resolution of *boundary layers*, and (4) control of *locking* phenomena. In the course of our discussion, we also consider related problems where p/hp versions have advantages, such as singularly perturbed second order elliptic PDEs, which can result in stronger boundary layers than the ones found in plate models.

2. *h*, *p* and *hp* finite element spaces

Suppose we are given a problem in variational form: Find $u \in V$ such that

$$B(u, v) = F(v), \quad v \in V. \tag{2.1}$$

Here F is a bounded linear functional on the (infinite dimensional) Hilbert space V, and $B(\cdot,\cdot)$ is a bounded, coercive, symmetric, bilinear form on $V \times V$. Then given a sequence of (finite element) subspaces $\{V_N\} \subset V$, we can define the finite element approximations $u_N \in V_N$ satisfying

$$B(u_N, v) = F(v), \quad v \in V_N. \tag{2.2}$$

It is easily shown that

$$\|u - u_N\|_{\mathrm{E}} \leqslant \inf_{v \in V_N} \|u - v\|_{\mathrm{E}}, \tag{2.3}$$

where $\|\cdot\|_{\mathrm{E}}$ is the *energy norm*

$$\|u\|_{\mathrm{E}} = (B(u,u))^{1/2}. \tag{2.4}$$

The coercivity and boundedness of B then gives

$$\|u - u_N\|_V \leqslant C \inf_{v \in V_N} \|u - v\|_V \tag{2.5}$$

but, as we shall see, the constant C in (2.5) can be large for some problems.

In all our examples, V will satisfy $H_0^1(\Omega) \subset V \subset H^1(\Omega)$[2] where $\Omega \subset \mathbb{R}^t$, $t = 1,2,3$ is a bounded domain with piecewise analytic boundary. The finite element spaces V_N will then consist of continuous piecewise polynomials defined on some mesh $\mathscr{T}_N$ on Ω. We describe these in more detail for the case $\Omega \subset \mathbb{R}^2$.

Assume each $\mathscr{T}_N$ is a regular [13] mesh consisting of straight-sided triangles and parallelograms $\{\tau_i^N\}$, $i=1,2,\ldots,I(N)$ (more general curvilinear elements could also be considered). For any element S, we define for $p \geqslant 0$ integer, $\mathscr{P}_p(S)$ ($\mathscr{Q}_p(S)$) to be the set of all polynomials of total degree (degree in each variable) $\leqslant p$. We also denote $\mathscr{Q}'_p(S) = \operatorname{span}\{\mathscr{P}_p(S), x^p y, x y^p\}$. Let $\boldsymbol{p}_N$ be a degree vector associating degree p_i^N to element τ_i^N (if p_i^N is independent of i, we write $\boldsymbol{p}_N = p_N$). Then the local polynomial spaces are denoted $\mathscr{R}_N(\tau_i^N)$ where $\mathscr{R}_N = \mathscr{P}_{p_i^N}$ if τ_i^N is a triangle and $\mathscr{R}_N = \mathscr{Q}_{p_i^N}$ or $\mathscr{Q}'_{p_i^N}$ if τ_i^N is a parallelogram. We then set

$$V_N = \{v \in V, v|_{\tau_i^N} \in \mathscr{R}_N(\tau_i^N)\}$$

($V_N \subset C^{(0)}(\Omega)$ for our examples).

Let us denote $h_i^N = \operatorname{diam}(\tau_i^N)$, $h_N = \max_i h_i^N$, $\underline{h}_N = \min_i h_i^N$. The sequence $\{\mathscr{T}_N\}$ is called *quasiuniform* provided there exists α independent of N such that

$$\frac{h_N}{\underline{h}_N} \leqslant \alpha.$$

As we shall see, spaces on quasiuniform meshes do not have the best properties where approximation of corner singularities is concerned. Rather, such singularities must be treated by nonquasiuniform mesh refinement, where the mesh becomes finer as one approaches the point of singularity. The type of mesh used in the hp version is *geometric*, and is defined below for the case of refinement towards the origin $\mathbf{O}$. (Fig. 1 gives a more intuitive idea than the definition, which is technical.)

Let $0 < q < 1$ be a number called the *geometric ratio*. Let $n(=n_N)$ be the number of layers around the origin $\mathbf{O}$. We denote the elements of $\mathscr{T}_N$ by $\tau_{n,j,k}^N$ where $j = 1,\ldots,\mu(k)$, $\mu(k) \leqslant \mu_0$ and $k = 1,2,\ldots,n+1$. Let $h_{n,j,k} = \operatorname{diam}(\tau_{n,j,k}^N)$ and $d_{n,j,k} = \operatorname{dist}(\tau_{n,j,k}^N, \mathbf{O})$. Then

(A) if $\mathbf{O} \notin \bar{\tau}_{n,j,k}^N$, for $j = 1,\ldots,\mu(k)$, $k = 2,\ldots,n+1$,

$$C_1 q^{n+2-k} \leqslant d_{n,j,k} \leqslant C_2 q^{n+1-k},$$

$$\kappa_1 d_{n,j,k} \leqslant h_{n,j,k} \leqslant \kappa_2 d_{n,j,k}.$$

[2] We use standard Sobolev space notation: $H^k(\omega)$ is the space of functions with k derivatives that are square integrable over ω. $H_0^1(\omega)$ is the subset of functions in $H^1(\omega)$ with vanishing trace on $\partial\omega$. $\|\cdot\|_{H^k(\omega)}$ is the norm of $H^k(\omega)$.

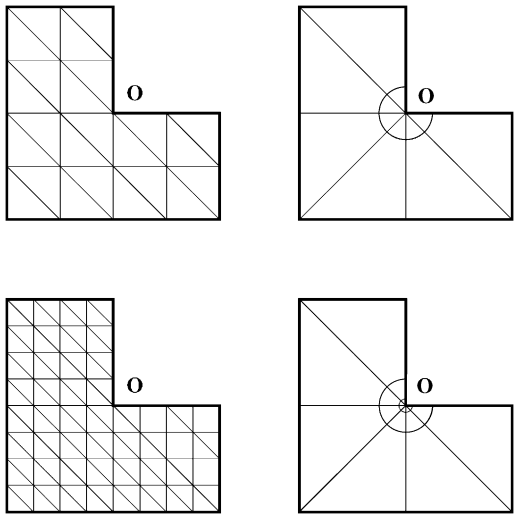

Fig. 1. Types of refinement: (a) quasiuniform, (b) geometric.

(B) if $\mathbf{O} \in \bar{\tau}^N_{n,j,k}$, then $k = 1$ and for $j = 1, \ldots, \mu(1)$,

$$\kappa_3 q^n \leqslant h_{n,j,k} \leqslant \kappa_4 q^n.$$

The constants C_i and κ_i are independent of N. See [21], where it is empirically shown that $q \approx 0.15$ is the best choice in terms of approximability. (In one dimension, this is theoretically established in [20].)

We can now talk about the following *extension procedures*, i.e. strategies for increasing the dimension of the space V_N to get a more accurate estimate in (2.3).

(i) *h version*: The most basic extension procedure consists of using quasiuniform meshes $\{\mathscr{T}_N\}$ with successively smaller h_N, with uniform $p_N = p$, kept fixed at $p = 1$ or 2 usually. Nonquasiuniform meshes (such as *radical* meshes, see [9]) could also be used.

(ii) *p version*: Here, $\mathscr{T}_N$ is the same for all N. Accuracy is achieved by increasing $\boldsymbol{p}_N$. The mesh could be uniform, but if a properly refined mesh (Fig. 1(b)) is used, the p version can often be made to yield the superior performance of the hp version (which is harder to implement).

(iii) *hp version*: Any $\{V_N\}$ for which both $\mathscr{T}_N$ and $\boldsymbol{p}_N$ are changed will give rise to an hp version. For instance, in Section 5, we consider an hp version designed to resolve boundary layers, where as $\boldsymbol{p}_N$ is increased, the number of elements remains the same, but the *size* of elements changes. For treating corner singularities, the geometric meshes with n layers described above are used, with p_N chosen uniformly to be $p_N = \kappa n_N$ (κ fixed), so that both p_N and n_N increase simultaneously. Even more efficient is the case that p_N is chosen to be the same over all elements in layer k, i.e. over all $\tau^N_{n,j,k}$ for $j = 1, \ldots, \mu(k)$, and increasing linearly with the index $k = 1, 2, \ldots, n + 1$ (see [21] for more details).

Let us mention that there are several differences between implementation of p/hp methods and the traditional h methods (for instance, the basis functions used in the p version are often not of nodal type). We do not discuss these aspects here but instead refer the reader to [40].

To conclude this section, we present the following theorem, which gives the basic estimate for the infimum in (2.5) when the norm $\|\cdot\|_V = \|\cdot\|_{H^1(\Omega)}$ and when the h, p or hp version over quasiuniform meshes is used.

Theorem 2.1 (Babuška and Suri [7]). *Let the spaces V_N consist of piecewise polynomials of degree p_N over a quasiuniform family of meshes $\{\mathcal{T}_N\}$ on $\Omega \subset \mathbb{R}^t$, $t = 1,2,3$. Then for $u \in H^k(\Omega)$, $k \geqslant 1$,*

$$\inf_{v \in V_N} \|u - v\|_{H^1(\Omega)} \leqslant C h_N^{\min(k-1,\, p_N)} p_N^{-(k-1)} \|u\|_{H^k(\Omega)} \tag{2.6}$$

with C a constant independent of u and N. (For a nonuniform distribution $\boldsymbol{p}_N$, we replace p_N by $\min(\boldsymbol{p}_N)$ *in* (2.6)).

Theorem 2.1 combined with (2.5) immediately shows that the following rates of convergence hold:

$$h \text{ version}: \quad \|u - u_N\|_V = \mathrm{O}(h_N^{\min(k-1,\, p_N)}), \tag{2.7}$$

$$p \text{ version}: \quad \|u - u_N\|_V = \mathrm{O}(p_N^{-(k-1)}). \tag{2.8}$$

Since the number of degrees of freedom $N \sim \mathrm{O}(h_N^{-t} p_N^t)$, we see that asymptotically, the rate of convergence (in terms of N) of the p version is never lower than that of the h version. In fact, for smooth solutions, it is often much better, as seen from (2.8) ("spectral" convergence). As we shall see in Section 4, the rate can be better even when the solution is not smooth.

3. Control of modeling error

Structural analysis over a three-dimensional domain (thin or otherwise) involves solving the equations of three-dimensional elasticity on the domain. When three-dimensional finite elements are used, the number of degrees of freedom N grows quite rapidly. For instance, while $N \sim \mathrm{O}(h^{-2})$ or $\mathrm{O}(p^2)$ in two dimensions (for the h and p versions, respectively), we have $N \sim \mathrm{O}(h^{-3})$ or $\mathrm{O}(p^3)$ in three dimensions. In the case that one dimension of the domain is thin, the three-dimensional model is often replaced by a two-dimensional model, formulated generally on the mid-plane of the domain. Discretization of this two-dimensional model then requires fewer degrees of freedom.

Let us present an illustrative example, that of a thin plate. Let ω be a bounded domain in $\mathbb{R}^2$ with piecewise smooth boundary, which represents the midplane of the plate, which we assume to be of thickness d ($d \ll \mathrm{diam}(\omega)$). Then, we represent the three-dimensional plate as

$$\Omega = \{x = (x_1, x_2, x_3) \in \mathbb{R}^3 \,|\, (x_1, x_2) \in \omega,\ |x_3| < d/2\}.$$

The lateral surface S and top and bottom surfaces $R_\pm$ are given by (see Fig. 2)

$$S = \{x \in \mathbb{R}^3 \,|\, (x_1, x_2) \in \partial\omega,\ |x_3| < d/2\},$$

$$R_\pm = \{x \in \mathbb{R}^3 \,|\, (x_1, x_2) \in \omega,\ x_3 = \pm d/2\}.$$

Let us denote the displacement $\boldsymbol{u} = (u_1, u_2, u_3)$. Then we consider the problem of finding $\boldsymbol{u} \in \boldsymbol{H}_D^1(\Omega) = \{\boldsymbol{u} \in (H^1(\Omega))^3 \,|\, u_3 = 0 \text{ on } S\}$ which satisfies

$$B(\boldsymbol{u}, \boldsymbol{v}) = F(\boldsymbol{v}) \ \forall \boldsymbol{v} \in \boldsymbol{H}_D^1(\Omega), \tag{3.1}$$

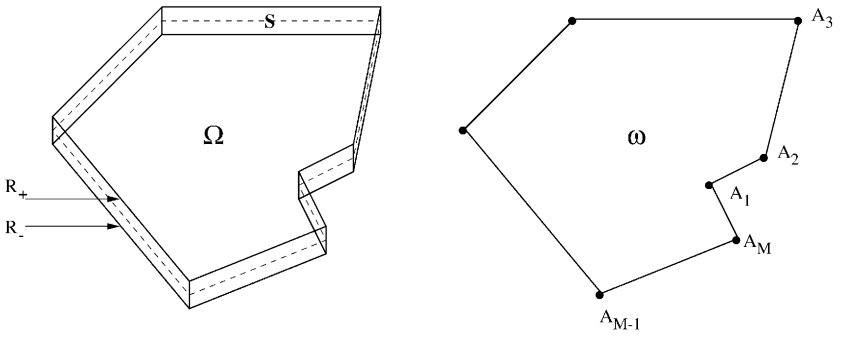

Fig. 2. The three-dimensional plate Ω and two-dimensional midplane ω.

where, with $t = 3$,

$$B(\boldsymbol{u},\boldsymbol{v}) = \frac{E}{1+\nu}\int_{\Omega}\left[\sum_{i,j=1}^{t}\varepsilon_{ij}(\boldsymbol{u})\varepsilon_{ij}(\boldsymbol{v}) + \frac{\nu}{1-2\nu}(\operatorname{div}\boldsymbol{u})(\operatorname{div}\boldsymbol{v})\right]\mathrm{d}x \tag{3.2}$$

and

$$F(\boldsymbol{v}) = \frac{1}{2}\int\int_{\omega} g(x_1,x_2)(v_3(x_1,x_2,d/2) + v_3(x_1,x_2,-d/2))\,\mathrm{d}x_1,\,\mathrm{d}x_2. \tag{3.3}$$

In the above, $E > 0$ is the Young's modulus of elasticity, $0 \leqslant \nu < \frac{1}{2}$ is the Poisson ratio and

$$\varepsilon_{ij}(\boldsymbol{u}) = \frac{1}{2}\left[\frac{\partial u_i}{\partial x_j} + \frac{\partial u_j}{\partial x_i}\right].$$

Eqs. (3.1)–(3.3) constitute the plate problem with *soft simple support* — we could use different constrained spaces to describe other physical problems (such as the *clamped* or *built-in* boundary condition which is obtained by using $\boldsymbol{u} = 0$ instead of $u_3 = 0$ on S).

Two-dimensional models are derived from (3.1)–(3.3) by making assumptions about the behavior of $\boldsymbol{u}$ with respect to the x_3 variable, substituting these into (3.1)–(3.3), and integrating in the x_3 variable to give a problem formulated on ω alone. The most basic classical plate model is the Kirchhoff–Love model, where we assume that

$$u_3(x_1,x_2,x_3) = w(x_1,x_2), \tag{3.4}$$

$$u_i(x_1,x_2,x_3) = -\frac{\partial w}{\partial x_i}(x_1,x_2)\left(\frac{x_3}{d/2}\right), \quad i = 1,2. \tag{3.5}$$

Substituting (3.4) and (3.5) into (3.1)–(3.3) and integrating in x_3, we get an equation for $w(x_1,x_2)$ alone, which is the weak form of the biharmonic problem.

One disadvantage of the KL model is that the corresponding variational form involves second derivatives of the FE functions, and hence requires $C^{(1)}$ continuous elements. The so-called Reissner–Mindlin (RM) model avoids this problem by replacing (3.5) by the expression

$$u_i(x_1,x_2,x_3) = \phi_i(x_1,x_2)\left(\frac{x_3}{d/2}\right), \quad i = 1,2. \tag{3.6}$$

Hence, we now have two more unknowns $(\phi_1, \phi_2) = \boldsymbol{\phi}$. This leads to the following variational form, after some modification of the elastic constants (see [5]): Find $U = (\boldsymbol{\phi}, w) \in V = H^1(\Omega) \times H^1(\Omega) \times H_D^1(\Omega)$ satisfying for all $W = (\boldsymbol{\theta}, \xi) \in V$,

$$B(U, W) = a(\boldsymbol{\phi}, \boldsymbol{\theta}) + \gamma\mu d^{-2}(\nabla w + \boldsymbol{\phi}, \nabla\xi + \boldsymbol{\theta}) = \int\int_{\omega} g\xi \, \mathrm{d}x_1 \, \mathrm{d}x_2, \tag{3.7}$$

where

$$a(\boldsymbol{\phi}, \boldsymbol{\theta}) = D \int\int_{\omega} \left\{ (1 - \nu) \sum_{i,j=1}^{2} \varepsilon_{ij}(\boldsymbol{\phi})\varepsilon_{ij}(\boldsymbol{\theta}) + \nu(\operatorname{div} \boldsymbol{\phi})(\operatorname{div} \boldsymbol{\theta}) \right\} \mathrm{d}x_1 \, \mathrm{d}x_2 \tag{3.8}$$

and where $D = E/12(1 - \nu^2)$, $\mu = E/2(1 + \nu)$ and γ is the shear correction factor.

It is seen from (3.7) that the RM model essentially enforces the Kirchhoff constraint,

$$KU = \nabla w + \boldsymbol{\phi} = 0 \tag{3.9}$$

in a penalized form (while the KL model enforces it *exactly*).

The replacement of the three-dimensional elasticity problem by a two-dimensional model such as RM leads to a *modeling error* between the actual three-dimensional solution and the solution obtained e.g. by (3.4)–(3.6). This modeling error is unaffected by any subsequent discretization of the two-dimensional model. The only way to decrease it is to use a more accurate model. To derive such more accurate models, we expand $\boldsymbol{u}(x_1, x_2, x_3)$ in terms of higher-order polynomials of x_3.

More precisely, let $n = (n_1, n_2, n_3)$ by a triple of integers $\geqslant 0$. We then make the ansatz (for $i = 1, 2$)

$$u_3(x_1, x_2, x_3) = \sum_{j=0}^{n_3} w_j(x_1, x_2) L_j\left(\frac{x_3}{d/2}\right), \tag{3.10}$$

$$u_i(x_1, x_2, x_3) = \sum_{j=0}^{n_i} \phi_{ij}(x_1, x_2) L_j\left(\frac{x_3}{d/2}\right), \tag{3.11}$$

which when substituted into the three-dimensional equations gives us the so-called $n = (n_1, n_2, n_3)$ model upon integration. (Here $\{L_j\}$ are the Legendre polynomials.) It is possible to show that (under some assumptions)

(1) For $n_1 \geqslant 1$, $n_2 \geqslant 1$, $n_3 \geqslant 2$, models $n = (n_1, n_2, n_3)$ converge, as $d \to 0$, to the same limiting solution as that obtained when $d \to 0$ in the three-dimensional elasticity equations. (For $n = (1, 1, 0)$, this is true with modified elastic constants.)
(2) For fixed d, as $\min(n_1, n_2, n_3) \to \infty$, the solutions of the models converge to the exact three-dimensional solution.

There are various factors such as boundary conditions, boundary layers, corner singularities, etc., which affect the convergence of a given model as $d \to 0$ [6]. For instance, in [17] it is shown that the RM model may not lead to good approximations of the boundary layer, while higher-order models significantly improve the convergence as $d \to 0$.

Let us denote for $n = (n_1, n_2, n_3)$

$${}^{n}H_D^1(\Omega) = \{\boldsymbol{u} = (u_1, u_2, u_3) \in H_D^1(\Omega) \text{ satisfying (3.10) and (3.11)}\}.$$

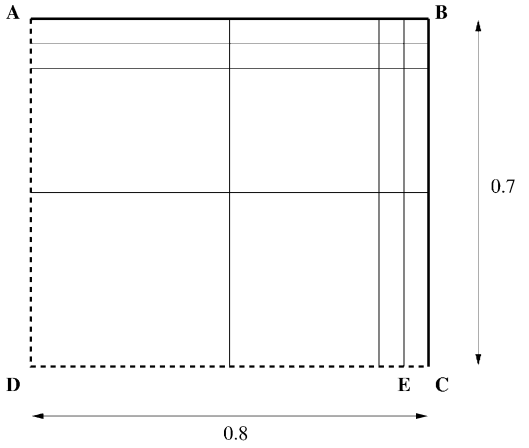

Fig. 3. Mid-plane of the quarter plate.

Then the solution of the (n_1, n_2, n_3) model can be expressed as the unique solution $\boldsymbol{u}^n$ of

$$B(\boldsymbol{u}^n, v) = F(\boldsymbol{v}) \quad \forall \boldsymbol{v} \in {}^nH_D^1(\Omega), \tag{3.12}$$

where B, F are as in (3.2) and (3.3). Eq. (3.12) represents a hierarchy of models of increasing accuracy.

Unfortunately, most finite element codes for plates (and shells) only discretize a *fixed* model of the above hierarchy (often the RM model, which is essentially the $(1,1,0)$ model — though sometimes the $(1,1,2)$ model is also used). This is generally the only option available in the h version. If, however, the code has p version capability, then it is possible to implement *hierarchical modeling* corresponding to (3.12) quite easily, provided the user can pick different polynomial degrees in different directions.

Assume that the midsurface ω is partitioned into elements $\{\tau_j\}$ which are either quadrilaterals or triangles. Then the domain Ω is partitioned into three-dimensional elements $\{T_j\} = \{\tau_j \times (-d/2, d/2)\}$. Let $R_j(p,q)$ be the corresponding polynomial space on T_j, where p is the degree in x_1, x_2 and q is the degree chosen in x_3. This space could be based on the choice $\mathscr{P}_p$, $\mathscr{Q}_p$ or $\mathscr{Q}'_p$ over τ_j in the (x_1, x_2) variables, and a (usually lower-degree) choice of q. Then, the corresponding FE solution with elements $R_j(p,q)$ of the three-dimensional plate problem will be exactly the same as the FE approximation (using elements of degree p) of the two-dimensional plate model (3.12) with $n_1 = n_2 = n_3 = q$. Hence, one can implement different plate models in the p/hp versions just by taking $q = 1, 2, 3, \ldots$, in the discretization of the three-dimensional elasticity problem (this hierarchic modeling is available, e.g., in the code STRESS CHECK). The modeling error may now be controlled.

Let us present a simple example using the code STRESS CHECK. Consider the quarter rectangular plate shown in Fig. 3, which has soft simple support conditions on AB, BC and symmetric conditions on CD, DA. The plate is subjected to a uniform outward transverse force of 1. Elastic constants are $E = 3.0 \times 10^7$ and $v = 0.3$, with shear correction factor of unity. The plate has thickness $=0.1$, which puts it in the "moderately thin" class — the mesh is designed so as to approximate the boundary layer well (see Section 5). We use the $n = (n, n, n)$ plate model with $n = 1, 2, 3$ and 6.

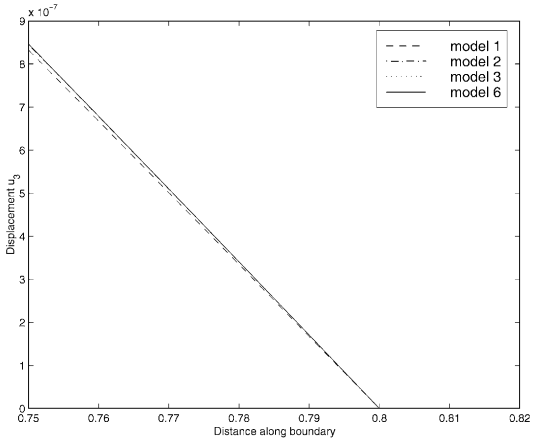

Fig. 4. Transverse displacement u_3 along EC for different models.

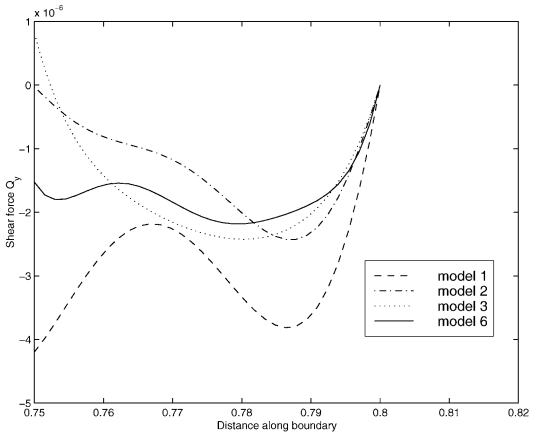

Fig. 5. Shear force distribution Q_y along EC for different models.

Figs. 4 and 5 show the extraction of two quantities — the transverse displacement u_3 and the shear force Q_y, along the lower edge of the element situated at the corner C. Degree $p = 8$ is used for the finite element approximations. It is observed that while there is no appreciable difference for u_3 with the model order, the quantity Q_y does vary appreciably. The reason for this is that u_3 has a very weak boundary layer, while Q_y has a stronger layer — and this is dependent on the model order (see [17] for more detailed experiments).

The above ideas also apply to other thin domains, such as composite plates and shells [10]. For these more complicated domains, the differences observed between different model orders is usually even more striking.

4. Approximation of singularities

The previous section showed how the three-dimensional elasticity equations over the plate Ω could be reduced to a hierarchy of elliptic problems (such as (3.7)) over the two-dimensional domain ω (Fig. 2(b)). It is well known that linear elliptic problems will (in general) have singularities at the corners A_j, $j = 1,\ldots,M$ of the domain ω, and also at points on $\partial\omega$ where the type of boundary condition changes, e.g., from Dirichlet to Neumann. For the three-dimensional problem over Ω, the singularities will occur not only at vertices of Ω but also along its edges. One of the main advantages of p/hp methods is that with proper mesh design, such singularities can be approximated very well.

4.1. A decomposition result

An examination of Eq. (3.7) shows that plate models such as the RM model are singularly perturbed in the variable ϕ. This results in boundary layers when d is small. The interaction of corner singularities and boundary layers is a complicated phenomenon, for which decomposition and regularity results may be found, e.g., in [25,16]. We will postpone the consideration of boundary layer approximation to Section 5. Here, to simplify the exposition, we assume that the thickness d is a fixed positive constant and do not worry about our approximation results being uniform in d.

Accordingly, given a linear elliptic problem on ω (which is one of our (n_1, n_2, n_3) models), we may use the results of Kondratiev (see [26] and also [19,15]) to decompose the solution in the neighborhood of any vertex A_j. If U is the solution and (r,θ) are the polar coordinates with origin at A_j, then we may write

$$U = \sum_{\ell=1}^{L}\sum_{s=0}^{S}\sum_{t=0}^{T} c_{\ell st}\psi_{\ell st}(\theta) r^{\alpha_\ell + t}\ln^s r + U_0$$

$$= \sum_{\ell=1}^{L} U_\ell + U_0 \tag{4.1}$$

in the neighborhood of A_j. Here $\psi_{\ell st}$ is a vector with the same number of components as U, and is analytic in θ. The exponents α_ℓ can be complex, and the coefficients $c_{\ell st}$ will depend on d. By taking L, S, T large enough, we can make U_0 as smooth as the data will allow. In fact, taking the correct number of terms near each A_j, we may write

$$U = \sum_{j=1}^{M}\sum_{\ell} U_\ell^{(j)}\chi_j + U_0, \tag{4.2}$$

where χ_j is a smooth cut-off function in the neighborhood of A_j and U_0 satisfies the appropriate shift theorem (e.g., in the case of (3.7), we would have

$$\|U_0\|_{[H^{k+2}(\omega)]^3} \leqslant C(d)\|g\|_{H^k(\omega)},$$

i.e., the same theorem as for a smooth boundary). Eqs. (4.1) and (4.2) show that when the finite element method is used, the rate of best approximation (i.e., the right side of (2.3)) will be determined by the worst singularity $\min_{\ell,j}|\alpha_\ell^{(j)}|$ (and the corresponding S in decomposition (4.1)), since the other terms (including U_0) are all smoother and hence result in better approximation rates.

4.2. hp convergence: quasiuniform meshes

We now present a theorem for the approximation of one of the canonical singularities present in (4.2), which we write as

$$u = r^{\alpha} \ln^{s} r\psi(\theta), \tag{4.3}$$

where ψ is a vector and for α complex, we understand r^{α} to denote $\operatorname{Re} r^{\alpha}$.

First, we note that for $\omega \subset \mathbb{R}^2$, $u \in H^{1+\hat{\alpha}-\varepsilon}(\omega)$ for any $\varepsilon > 0$, where $\hat{\alpha} = \operatorname{Re}\alpha$. We could apply Theorem 2.1 to get an approximation rate of $O(h_N^{\min(\hat{\alpha}-\varepsilon,\, p_N)} p_N^{-\hat{\alpha}+\varepsilon})$, but as shown in [7], this result can be improved to give the following theorem.

Theorem 4.1. *Let u be given by* (4.3). *Let quasiuniform meshes be used. Then*

$$\inf_{v \in V_N} \|u - v\|_{H^1(\omega)} \leqslant Ck(h_N, p_N, s) \min\left\{ h_N^{\hat{\alpha}}, \frac{h^{\min(\hat{\alpha},\, p_N - \hat{\alpha})}}{p_N^{2\hat{\alpha}}} \right\}, \tag{4.4}$$

where $k(h_N, p_N, s) = \max(|\ln^{s} h_N|, |\ln^{s} p_N|)$ and C is a constant independent of N.

Theorem 4.1 shows that one gets the following convergence rates:

$$h \text{ version}: \ O(h_N^{\hat{\alpha}}), \tag{4.5}$$

$$p \text{ version}: \ O(p_N^{-2\hat{\alpha}}). \tag{4.6}$$

Since $N = O(h_N^{-2} p_N^2)$, we see that the p version gives *twice* the convergence rate of the h version. This happens whenever the point of singularity $r = 0$ coincides with the node of an element. If the singularity point lies in the interior of an element, then the doubling effect does not take place.

Applying Theorem 4.1 to each component of (4.2) and assuming that U_0 is smooth enough to be better approximated, we see that (4.4)–(4.6) will also hold for the error $\|U - U_N\|_V$ where U_N is the FEM approximation to U.

4.3. hp convergence: nonquasiuniform meshes

For the h version with polynomials of fixed degree p, it is well known that the optimal convergence rate for smooth functions is $O(h_N^p)$. Hence, the rate (4.5) can be quite far from optimal if $\hat{\alpha}$ is small (for example, $\hat{\alpha} < 1$ in nonconvex domains for the Poisson equation). It turns out that the use of nonquasiuniform meshes, which are increasingly refined towards the points of singularity, can increase the convergence rate. The optimal meshes in this regard are the so-called *radical* meshes, which result in $O(h_N^p)$ convergence for function (4.3) when the mesh is designed taking into account the strength of the singularity $\hat{\alpha}$ and the degree of the polynomial p. We refer to [20] where a full analysis of such meshes is given in one dimension and to [4] where the case $p = 1$ is analyzed in two dimensions.

Here, we present a result for the hp version, which shows that with the *geometric* meshes described in Section 2, one obtains *exponential* convergence in terms of N, the number of degrees of freedom (note that $O(h_N^p)$ convergence is only *algebraic* in N). The spaces V_N are chosen as follows. In the vicinity of each singularity point, a geometric mesh with n_N layers (see Section 2) is constructed,

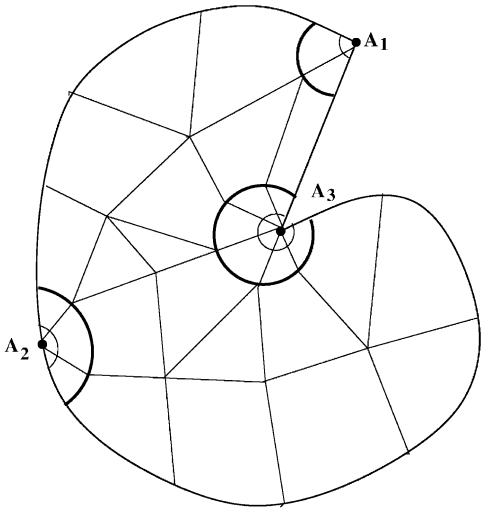

Fig. 6. hp mesh with $n_N = 2$ layers. A_2 is a singularity point where the type of boundary condition changes.

such that these meshes conform with a fixed mesh over the remainder of the domain (see Fig. 6). The (uniform) degree p_N is chosen to be κn_N over all elements on the domain. As N increases, n_N is increased (and hence so is p_N). The increase in the number of layers causes the singularities to be better approximated. The smooth parts are well-approximated by the increase in p_N.

Theorem 4.2. *Let U be the solution of the RM model* (3.7), (3.8). *Let V_N be the hp spaces described above. Then*

$$\inf_{W \in V_N} \|U - W\|_V \leqslant C\mathrm{e}^{-\gamma \sqrt[3]{N}} \tag{4.7}$$

with C a constant independent of N.

The bound in estimate (4.7) in one dimension becomes $C\mathrm{e}^{-\gamma\sqrt{N}}$ [20], while in three dimensions it is $C\mathrm{e}^{-\gamma \sqrt[5]{N}}$ [3]. The design of geometric meshes in three dimensions is described further in [3]. The constant C in Eq. (4.7) will depend on d.

4.4. Numerical example

We illustrate some of the results of the past two theorems, by considering the bending of the L-shaped plate shown in Fig. 1. The longest side of the plate is taken to be 0.8, with $d = 0.1$, $E = 3.0 \times 10^7$, $v = 0.3$, $\gamma = 1$. A uniform $g = 1$ is applied, and the plate is *clamped* ($\boldsymbol{u} = 0$) along the entire boundary.

Fig. 7 shows the percentage relative energy norm error when various h and p versions are used. (The true energy was estimated by using a much larger number of degrees of freedom.) It is observed that with the h version on meshes of the type shown in Fig. 1(a), the error decreases algebraically. For the p version on a uniform mesh of only 6 triangles (i.e., no geometric refinement layers

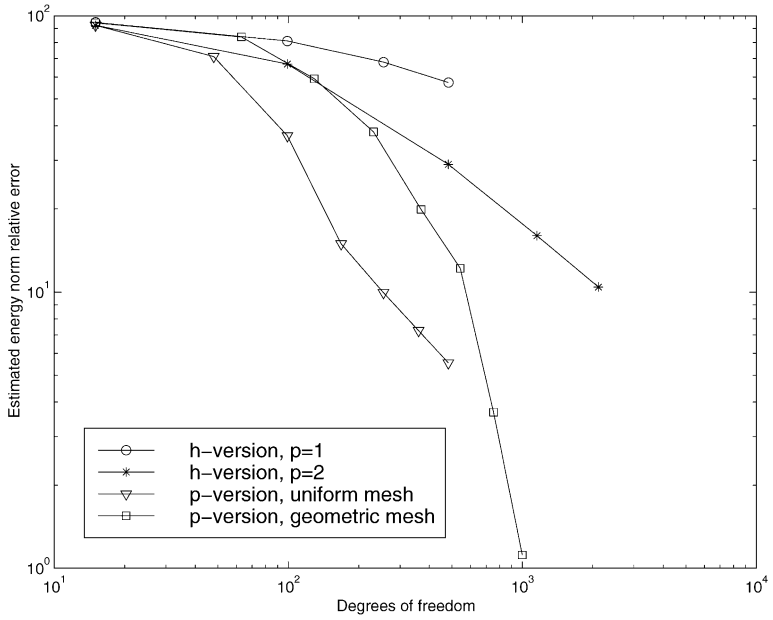

Fig. 7. Error curves for h and p versions.

in Fig. 1(b)), the error follows an 'S' curve, with the middle portion representing an exponential decrease, and the flat portion representing twice the algebraic h version rate. When one layer of mesh refinement is introduced (as in the top of Fig. 1(b)), it is observed the exponential rate continues through $p = 8$. Further mesh refinement would only be useful when this graph flattens out as well — essentially, in the range of parameters shown, the p version is displaying the same exponential rate of convergence expected from the hp version. For more detailed experiments, we refer, e.g., to [7].

5. Resolution of boundary layers

If one lets $d \to 0$ in Eqs. (3.1)–(3.3), then one gets a system of *singularly perturbed* equations [16]. This will also be true for the (n_1, n_2, n_3) model given by (3.12). For instance, it is clear from (3.7) and (3.8) that the RM model is singularly perturbed in $\boldsymbol{\phi}$ (but not in w), since multiplying (3.7) through by d^2, the order of derivatives in $\boldsymbol{\phi}$ decreases to 0 as $d \to 0$. This implies that for most boundary conditions $\boldsymbol{\phi}$ will have a *boundary layer* at $\partial\omega$ for small d, i.e., components in the solution of the form (Fig. 8)

$$\boldsymbol{\phi}_{\mathrm{b}}(s,t) = C(d)\boldsymbol{f}(t)\mathrm{e}^{-ks/d}. \tag{5.1}$$

Here (s,t) are local coordinates in the normal and tangential directions at $\partial\omega$, k is a constant and $\boldsymbol{f}$ is a smooth function. The amplitude $C(d)$ of the boundary layer will depend upon the type of boundary conditions — for instance, the largest amplitude $C(d) = \mathrm{O}(d)$ occurs for the case of the soft simple support and free plates, while for clamped (built-in) conditions, it is only $\mathrm{O}(d^2)$ [1].

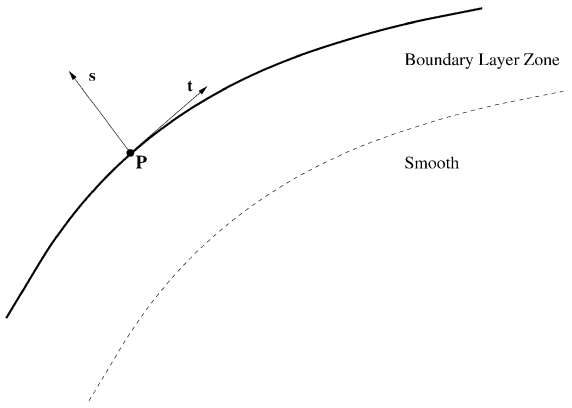

Fig. 8. The boundary layer.

The amplitude will have the same *order* (though not the same value [17]) for all (n_1, n_2, n_3) plate models. The only model free of boundary layers is the KL model. For a discussion of the relation of boundary layers in the three-dimensional case to those in (n_1, n_2, n_3) models, we refer to [17].

Our concern in this section is the *approximation* of components such as (5.1) by the FEM. We note that the boundary layer effect is essentially a one-dimensional effect, so that if we can efficiently approximate the functions $\boldsymbol{\phi}_{\mathrm{b}}$ in the normal direction, then we can expect to have an overall good approximation. Our first step, therefore, is to consider the approximation of the one-dimensional boundary layer function

$$\bar{u}_d(x) = \mathrm{e}^{-x/d} \tag{5.2}$$

by the space V_N of piecewise polynomials of degree $\boldsymbol{p}_N = (p_1^N, p_2^N, \ldots, p_I^N)$ on the mesh $\mathscr{T}_N = \{0 = x_0 < x_1, \ldots, < x_I = 1\}$.

Let us consider the approximation of (5.2) in the context of the one-dimensional singularly perturbed problem

$$-d^2 u_d''(x) + u_d(x) = f(x), \quad x \in I = (-1, 1), \tag{5.3}$$

$$u_d(\pm 1) = \alpha^{\pm}. \tag{5.4}$$

It is well known (see, e.g., [33]) that the solution of (5.3) and (5.4) can be decomposed as

$$u_d(x) = u_d^{\mathrm{s}} + A_d \bar{u}_d(1 + x) + B_d \bar{u}_d(1 - x), \tag{5.5}$$

i.e., it contains terms of form (5.2), plus a smooth (in d) component u_d^{s}. Writing (5.3) and (5.4) in variational form, we have that $u_d \in H_0^1(I)$ satisfies $\forall v \in H_0^1(I)$,

$$B_d(u_d, v) := \int_I \{d^2 u_d' v' + u_d v\}\,\mathrm{d}x = \int_I f v\,\mathrm{d}x. \tag{5.6}$$

We consider the approximation of $\bar{u}_d$ in the energy norm for (5.6), i.e., in the norm

$$\|v\|_d = (B_d(v, v))^{1/2} \approx d\|v'\|_{L_2(I)} + \|v\|_{L_2(I)}.$$

For the h version on a quasiuniform mesh, we may apply (2.6), together with an L_2 duality result, to obtain (for $k \geqslant p_N + 1$)

$$\inf_{v \in V_N} \|\bar{u}_d - v\|_d \leqslant C h_N^{k-1} d^{-k+3/2}, \tag{5.7}$$

where we have used (5.2) to estimate $\|\bar{u}_d\|_{H^k(I)}$. We see that for fixed d, we get the optimal $O(h_N^{k-1})$, but as $d \to 0$, this rate deteriorates. The best possible *uniform* rate for $0 < d \leqslant 1$ is $O(h_N^{1/2})$, obtained by taking $k = \frac{3}{2}$. This is the rate observed in practice for d small.

For the p version, it is shown in [33] that the following theorem holds. Here, $\tilde{p} := p + \frac{1}{2}$.

Theorem 5.1. (A) *Let* $r = (e/2\tilde{p}_N d) < 1$. *Then*

$$\inf_{v \in V_N} \|\bar{u}_d - v\|_d \leqslant C d^{1/2} r^{\tilde{p}_N} (1 - r^2)^{-1/2}, \tag{5.8}$$

where C *is a constant independent of* p_N *and* d.

(B) *We have*

$$\inf_{v \in V_N} \|\bar{u}_d - v\|_d \leqslant C p_N^{-1} \sqrt{\ln p_N}, \tag{5.9}$$

uniformly for $0 < d \leqslant 1$.

Theorem 5.1 shows that while rate (5.8) is exponential, it only holds for p_N very large (not generally seen in practice). The best uniform rate is given by (5.9), and is *twice* that for the h version (modulo the log factor).

Estimates (5.7) and (5.9) show that both the h and p versions give disappointing convergence rates uniform in d. One remedy for this is to use nonquasiuniform meshes, by which the $O(h_N^{k-1})$ rate of the h version can be recovered. One such mesh is given in [33], by $\mathscr{T}_N = \{-1, x_1, \ldots, x_{m-1}, 1\}$, where, for m even, and $p_N \equiv p$,

$$x_{m/2 \pm i} = \mp d\,\tilde{p} \ln(1 - 2ic/m), \quad i = 0, \ldots, m/2 \tag{5.10}$$

with $c = 1 - \exp(1 - 1/(d\,\tilde{p}))$. See, e.g., [35,43] for other examples.

Another solution, possible when both h and p capability is available, is to insert a single element of size $O(\tilde{p}d)$ at the boundary layer, and let $p \to \infty$. This gives exponential convergence. More precisely, the following theorem is established in [33].

Theorem 5.2. *Let* $(\mathscr{T}_N, \boldsymbol{p}_N)$ *be such that for* $p \geqslant 1$,

$$\boldsymbol{p}_N = \{p, 1\}, \quad \mathscr{T}_N = \{-1, -1 + \kappa\tilde{p}d, 1\} \quad \text{if } \kappa\tilde{p}d < 2,$$

$$\boldsymbol{p}_N = \{p\}, \quad \mathscr{T}_N = \{-1, 1\} \quad \text{if } \kappa\tilde{p}d \geqslant 2, \tag{5.11}$$

where $0 < \kappa_0 \leqslant \kappa < 4/e$ *is a constant independent of* p *and* d. *Then with* $\bar{u}_d = \bar{u}_d(x + 1)$, *there exists* $0 < \alpha < 1$ *such that*

$$\inf_{v \in V_N} \|\bar{u}_d - v\|_d \leqslant C d^{1/2} \alpha^{\tilde{p}}$$

with C, α *independent of* p *and* d.

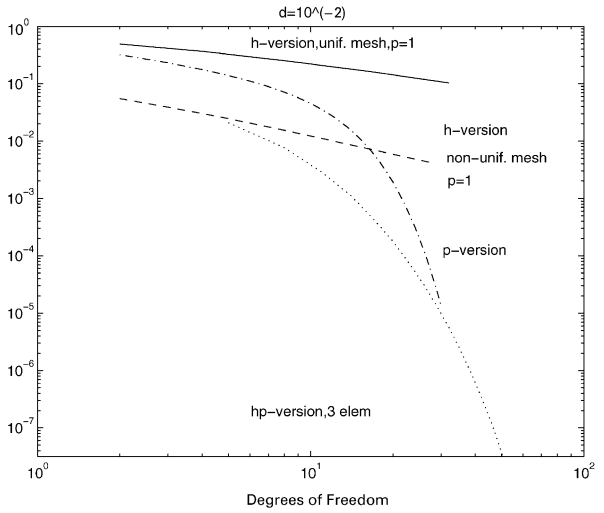

Fig. 9. Comparison of various methods, $d = 10^{-2}$.

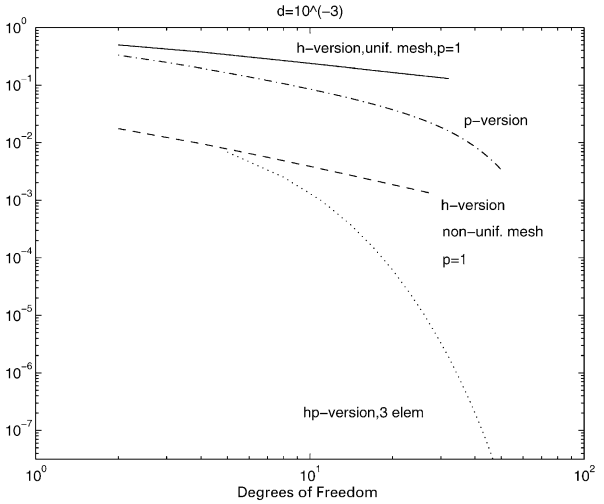

Fig. 10. Comparison of various methods, $d = 10^{-3}$.

We see from the above construction that what we have is an hp method, since the mesh changes as $p \to \infty$. (Experiments indicate that remeshing can be avoided by fixing $\mathscr{T}_N = \{-1, -1+\kappa \tilde{p}_{\max} d, 1\}$ in many cases.)

In Figs. 9 and 10, we compare four different methods discussed above, including the h version given by (5.10) (with $p = 1$), and the hp version described in Theorem 5.2. In each case, we treat problem (5.3), (5.4), with $f(x) = 1$, $\alpha^{\pm} = 0$. Since the solution has boundary layers at both end points of I, we must now refine near both end points, so that, e.g., instead of (5.11), we get the three-element mesh $\{-1, -1+\kappa \tilde{p} d, 1-\kappa \tilde{p} d, 1\}$. The superiority of the hp version is clearly noticed for d small.

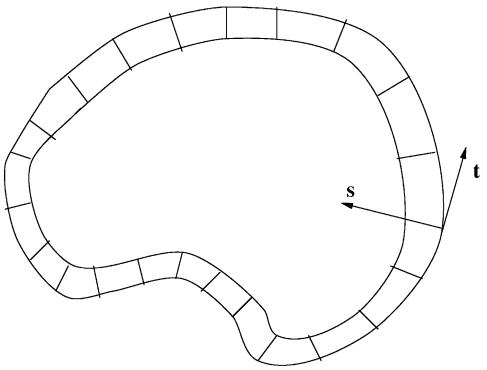

Fig. 11. Boundary-fitted mesh.

The above effect may also be observed for two-dimensional problems. Consider the singularly perturbed problem

$$-d^2\,\Delta u + u = f \quad \text{in } \omega, \tag{5.12}$$

$$u = 0 \quad \text{on } \partial\omega. \tag{5.13}$$

If ω is a smooth domain, then the solution will again have a component of the form (5.1), with $C(d) = \mathrm{O}(1)$. If we now construct a mesh in boundary-fitted coordinates (s,t), such that the (tensor product) basis functions are polynomials in s multiplied by polynomials in t, then the problem of approximating (5.1) reduces once more to a one-dimensional approximation. Hence, for example, we should take the mesh to be such that in the s direction, the first layer of elements is of $\mathrm{O}(\kappa\tilde{p}d)$ (see Fig. 11). Then one can again establish exponential hp convergence for the solution of (5.12) and (5.13) uniform in d [44,45,27]. This may also be done when the meshes and basis functions are suitably fitted in (x,y) rather than (s,t) coordinates, as long as the $\mathrm{O}(\kappa\tilde{p}d)$ layer character is maintained.

In Figs. 13 and 14, we show experiments performed using STRESS CHECK for (5.12) and (5.13) on the unit circle, with $f = 1$, for which the exact solution can be expressed in terms of a modified Bessel function (Eq. (7.2) of [45]) and has a boundary layer at $\partial\omega$. We take $p_{\max} = 8$ and perform the p version on the two meshes shown in Fig. 12. The first approximates the one from Theorem 5.2, with a layer of elements of size $p_{\max}d$, while the second is a more uniform mesh, fixed for all d. The advantage of the first mesh is clearly demonstrated in Figs. 13 and 14.

The case of a nonsmooth domain is more subtle. For instance, if ω is a polygon, then the singularities for (5.12) and (5.13) now behave essentially like $(r/d)^{\alpha}$ [24]. Consequently, the mesh refinement for the singularities must now be carried out in an $\mathrm{O}(d)$ region of the corners, as shown in Fig. 15. In [47], *spectral* convergence of $\mathrm{O}(p^{-k})$, k arbitrary, has been established for such meshes as $p \to \infty$.

For the case of the RM plate, as noted before, the strongest boundary layer (in the case of the free or the soft simply supported plate) is only $\mathrm{O}(d)$. Consequently, the refinement of the singularities (i.e., usual $\mathrm{O}(1)$ hp refinement) is usually sufficient in practice when the error in the energy norm is of interest. However, if quantities involving the s-derivative of (5.1) are calculated (such as

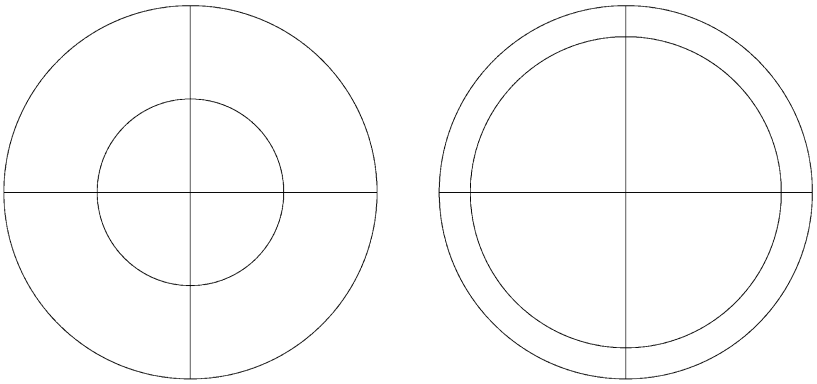

Fig. 12. The two meshes.

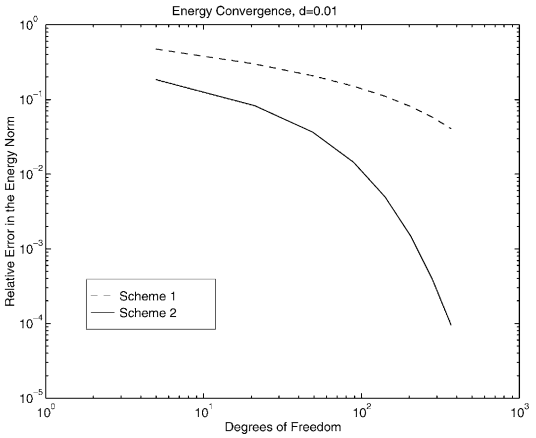

Fig. 13. Comparison of p version, $d = 10^{-2}$.

moments), then these will again contain an O(1) boundary layer, and refinements such as that in Fig. 15 will again be necessary (recall the example in Fig. 3, see, e.g., [34,46]).

For shell problems, the solutions have a rich array of boundary layers, which are often stronger than those encountered in plates. Ideas similar to the ones discussed above may be applied to such problems as well. We refer to [23,29,18,22] for some results.

6. The problem of locking

There is one more problem that occurs in the numerical approximation of thin domains, that of *numerical locking*. Consider once again the RM model (3.7). As $d \to 0$, we see that for the energy norm $\|U\|_{\mathrm{E},d} = (B(U,U))^{1/2}$ to remain finite, we must have the Kirchhoff constraint (3.9) to be satisfied in the limit. This just expresses the fact that the RM model converges to the KL model in energy norm.

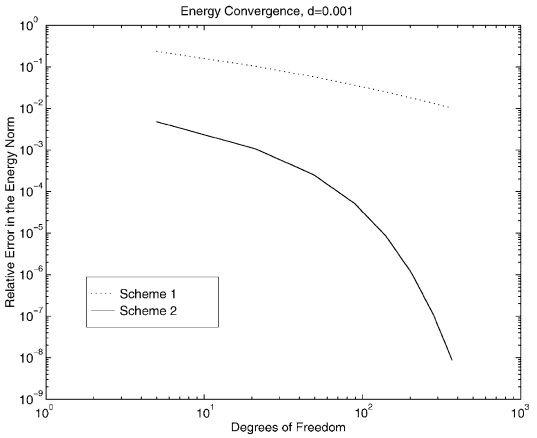

Fig. 14. Comparison of p version, $d = 10^{-3}$.

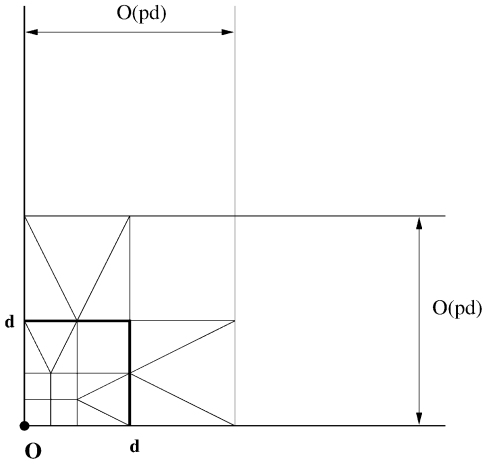

Fig. 15. The mesh for polygons.

If we now consider the finite element approximation of (3.7), then the finite element solution $U_N = (\boldsymbol{\phi}_N, w_N)$ must *also* satisfy (3.9) in the limit $d \to 0$ to keep the energy norm $\|U_N\|_{\mathrm{E},d}$ finite, i.e.,

$$KU_N = \nabla w_N + \boldsymbol{\phi}_N = 0. \tag{6.1}$$

As a result, only those functions $U_N \in V_N$ satisfying (6.1) will be relevant in approximating U in the limit. The quasioptimality estimate (2.3) must now be replaced by [8]

$$\|U - U_N\|_{\mathrm{E}} \leqslant \inf_{\substack{Y \in V_N \\ KY = 0}} \|U - Y\|_{\mathrm{E}}, \tag{6.2}$$

which is the best estimate that holds for $\|\cdot\|_{\mathrm{E}} = \|\cdot\|_{\mathrm{E},0}$.

Defining $S^K = \{Y \in S,\ KY = 0\}$ for any space $S \subset V$, we see that the infimum in (6.2) is taken not over V_N but over a proper subset V_N^K. *Locking* ("shear" locking) is said to occur when this causes a deterioration in the resulting approximation.

One way of understanding this deterioration is to note that (6.1) essentially forces W_N to be a $C^{(1)}(\omega)$ function (since $\boldsymbol{\phi}_N$ must lie in $H^1(\omega)$, i.e., W_N must be in $H^2(\omega)$). This, of course, is consistent with the fact that in the $d=0$ limit, we are approximating the fourth-order KL (biharmonic) problem, for which, as noted earlier, $C^{(1)}$ functions are needed for W_N. Suppose, for instance, we choose $V_N = S_N \times Z_N$ where S_N, Z_N both contain continuous piecewise linears. Then $(\boldsymbol{\psi}_N, z_N) \in V_N^K$ only if $z_N \in C^{(1)}(\omega)$, so that z_N will be a linear function over *all* of ω. If, for instance, we have built-in boundary conditions, then $z_N = 0$ will be the only function satisfying this requirement in Z_N, and the finite element solution $(\boldsymbol{\phi}_N, w_N)$ will be such that w_N is forced to converge to 0 as $d \to 0$. This is an example of *complete* locking, where there is *no* uniform rate of convergence. For other choices of spaces, locking may manifest itself as a degradation (but perhaps not a complete annihilation) of the uniform convergence rate.

A formal definition of locking may be found in [8]. The definition involves several factors. First, we are given a sequence of problems $\{P_d\}$ dependent on a parameter d in some set $S = (0, 1]$ (say). For thin domains, d is, of course, the thickness. For linear elasticity, we could take $d = 1 - 2\nu$, with ν= Poisson's ratio. Next, we assume that the solution u_d to P_d lies in the solution space H_d — this characterizes the smoothness of the exact solutions $\{u_d\}$. Also, we are given a sequence of finite element spaces $\{V_N\}$ that comprise an extension procedure $\mathscr{F}$. Finally, we are interested in the errors $E_d(u_d - u_{d,N})$ where $u_{d,N} \in V_N$ is the FE solution and E_d is some given error functional (e.g., the energy norm, the $H^1(\Omega)$ norm, etc.).

We now define a function $L(d, N)$ called the *locking ratio* by

$$L(d,N) = \frac{\sup_{u_d \in H_d^B} E_d(u_d - u_{d,N})}{\inf_{d \in S_\alpha} \sup_{u_d \in H_d^B} E_d(u_d - u_{d,N})} \tag{6.3}$$

where $S_\alpha = S \cap [\alpha, \infty)$ for some $\alpha > 0$ such that $S_\alpha \neq \phi$. Here $H_d^B = \{u \in H_d,\ \|u\|_{H_d} \leqslant B\}$.

What $L(d, N)$ does is to compare the performance of the method at thickness $= d$ to the best possible performance for values of $d \geqslant \alpha$ for which locking does not occur. If S is restricted to a discrete set, it gives a *computable* measure of the amount of locking [37].

An alternative definition of locking can be based on the asymptotic rate of convergence [8]:

Definition 6.1. The extension procedure $\mathscr{F}$ is free from locking for the family of problems $\{P_d\}$, $d \in S = (0, 1]$ with respect to the solution sets H_d and error measures E_d, if and only if

$$\limsup_{N \to \infty} \left(\sup_{d \in (0,1]} L(\nu, N) \right) = C < \infty.$$

$\mathscr{F}$ shows locking of order $f(N)$ if and only if

$$0 < \limsup_{N \to \infty} \left(\sup_{\nu} L(\nu, N) \frac{1}{f(N)} \right) = C < \infty$$

where $f(N) \to \infty$ as $N \to \infty$. It shows locking of at least (respectively, at most) order $f(N)$ if $C > 0$ (respectively, $C < \infty$).

Let us make a second definition, that of robustness:

Definition 6.2. The extension procedure $\mathscr{F}$ is robust for $\{P_d\}$, $d \in S=(0,1]$ with respect to solution sets H_d and error measures E_d if and only if

$$\lim_{N\to\infty} \sup_{d} \sup_{u_d\in H_d^B} E_d(u_d - u_{d,N}) = 0.$$

It is robust with uniform order $g(N)$ if and only if

$$\sup_{d} \sup_{u_d\in H_d^B} E_d(u_d - u_{d,N}) \leqslant g(N),$$

where $g(N) \to 0$ as $N \to \infty$.

We now discuss locking and robustness for the plate problem in the context of the above definitions. In order to concentrate solely on the issue of locking, we consider *periodic* boundary conditions, for which no boundary layers exist, and the solution is smooth. For $\omega = (-1,1)^2$, these conditions are given by

$$U_d(x_1,1) = U_d(x_1,-1), \quad U_d(1,x_2) = U_d(-1,x_2), \ \ |x_1|,|x_2| \leqslant 1 \tag{6.4}$$

so that $V = [H^1_{\text{per}}(\omega)]^3$ where $H^k_{\text{per}}(\omega)$ denotes the set of functions on ω whose periodic extensions to $\mathbb{R}^2$ lie in $H^k_{\text{loc}}(\mathbb{R}^2)$.

Let us consider Definitions 6.1 and 6.2 for the case that the error measure $E_d \equiv \|\cdot\|_{\text{E},d}$ (the energy norm corresponding to (3.7)). For our solution sets, we take

$$H_d = \{U = (\boldsymbol{\phi}, w),\ \boldsymbol{\phi} \in H^{k+1}_{\text{per}}(\omega), C_d U = 0\}, \tag{6.5}$$

where

$$C_d U = \frac{d^2}{12(1-\nu)}\{(1-\nu)\Delta\boldsymbol{\phi} + (1+\nu)\nabla\nabla\cdot\boldsymbol{\phi}\} + \frac{\gamma}{2(1+\nu)}\{\nabla w + \boldsymbol{\phi}\}.$$

The constraint in (6.5) says that $U \in H_d$ satisfies the first equation in the usual strong form of (3.7).

We then have the following two theorems [39].

Theorem 6.3. *Let $\mathscr{F}$ be an h version extension procedure on a uniform mesh consisting either of triangles or rectangles, for problem* (3.7), (6.4). *Let polynomials of degree $p = p_N$ and $q = q_N$ be used for the rotations $\boldsymbol{\phi}_d$ and displacements w_d respectively. Then with solution sets H_d and error measures $\|\cdot\|_{\text{E},d}$, $\mathscr{F}$ is robust with uniform order $N^{-\ell}$ when $k \geqslant 2q+1$ and shows locking of order N^r when $k \geqslant p+1$, as summarized in Table* 1.

Theorem 6.4. *Let $\mathscr{F}$ be the p version on a mesh of triangles and parallelograms, with $p_N \geqslant 1$, $q_N \geqslant p_N$. Then with solution sets $H_d, k \geqslant 1, \mathscr{F}$ is free of locking in the energy norm and is robust with uniform order $N^{-(k-1)/2}$ as $p_N \to \infty$.*

Remark 6.5. The hp version will also be free of locking, provided (uniform) triangular meshes with $p_N \geqslant 5$ and $q_N \geqslant p_N + 1$ are used (Theorem 5.2 of [39]).

Table 1
Locking and robustness for the h version with uniform meshes

Type of element	Degree p	Degree q	Order of locking, r $f(N)=\mathcal{O}(N^r)$	Robustness order, l $g(N)=\mathcal{O}(N^{-l})$
Triangle ($\mathscr{P}_p$)	1	$q\geqslant 1$	$r=\frac{1}{2}$	$l=0$
	$2\leqslant p\leqslant 4$	$q=p$	$r=1$	$l=(p-2)/2$
	$p\geqslant 5$		$r=\frac{1}{2}$	$l=(p-1)/2$
	$2\leqslant p\leqslant 3$	$l\geqslant p+1$	$r=\frac{1}{2}$	$l=(p-1)/2$
	$p\geqslant 4$	$l\geqslant p+1$	$r=0$	$l=p/2$
Product ($\mathscr{Q}_p$)	1	$l\geqslant 1$	$r=\frac{1}{2}$	$l=0$
	$p\geqslant 2$	$q\geqslant p$	$r=\frac{1}{2}$	$l=(p-1)/2$
Trunk ($\mathscr{Q}'_p$)	1	$q\geqslant 1$	$r=\frac{1}{2}$	$l=0$
	2	$q=2,3$	$r=1$	$l=0$
		$q\geqslant 4$	$r=\frac{1}{2}$	$l=1/2$
	$p\geqslant 3$	$q=p$	$r=\frac{3}{2}$	$l=(p-3)/2$
		$q\geqslant p+1$	$r=1$	$l=(p-2)/2$

Let us briefly explain the idea behind Theorems 6.3 and 6.4. Suppose $F_0(N)$ represents the *optimal* rate of convergence for $\mathscr{F}$ in the absence of locking. For example, $F_0(N)$ would behave like the $\|\cdot\|_{\mathrm{E},d}$ error when d is set equal to 1. Let us also define

$$g(N)=\sup_{w\in H^{k+2,B}_{\mathrm{per}}}\inf_{z\in W_N}\|w-z\|_{H^2(\omega)} \tag{6.6}$$

where for $V_N=S_N$, $W_N=\{w\in Z_N, \operatorname{grad} w\in S_N\}$. Then it can be shown quite easily [39] that $\mathscr{F}$ is robust with uniform order $\max\{F_0(N),g(N)\}$ and shows locking of order $f(N)$ if and only if

$$C_1F_0(N)f(N)\leqslant g(N)\leqslant C_2F_0(N)f(N).$$

(The characterization (6.6) follows easily if we remember that $\boldsymbol{\phi}_d=\nabla w_d$, $\boldsymbol{\phi}_{d,N}=\nabla w_{d,N}$ in the limit $d\to 0$.)

Now the question of locking becomes one in pure approximation theory. For instance, it is known that to get optimal h-approximation over triangles using $C^{(1)}$ elements, one must use at least degree 5 piecewise polynomials, which shows why in Table 1, the locking disappears only when $q\geqslant 5$ is used for Z_N. In the p version, on the other hand, since we have p_N, $q_N\to\infty$, the condition $q_N\geqslant 5$ will not cause any problem asymptotically. Hence, in the asymptotic sense, there will be no locking, though as seen from Fig. 17 ahead, there *is* a shift in the error curves (i.e., there will be an increase in the locking ratios).

In Figs. 16 and 17, we illustrate the above rates of convergence for problem (3.7), (6.4) on $\omega=(-1,1)^2$. The Poisson ratio $v=0.3, E=1$, and the load is $g(x,y)=\cos(\pi x/2)\cos(\pi y/2)$. A uniform rectangular mesh is used with $p=q$ product spaces, and the errors presented are those estimated by STRESS CHECK.

Fig. 16 clearly shows the locking of $\mathrm{O}(N^{1/2})$. Fig. 17 shows the parallel error curves for the p version, indicating an absence of asymptotic locking (but also indicating locking ratios $L(d,N)>1$).

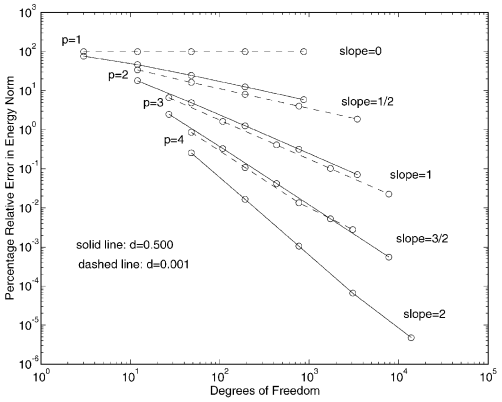

Fig. 16. The h version for the RM plate.

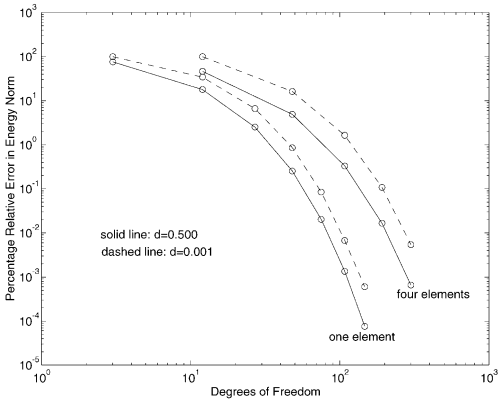

Fig. 17. The p version for the RM plate.

Let us remark now on some extension of these results:

1. *Non-periodic boundary conditions*: Similar results were observed computationally for clamped (built-in) plates. The locking theorems above will hold once more, provided the solution is smooth. But in general, it is not, and boundary layer effects must also be considered [32,5].

2. *Higher-order plate models*: In [39], it is shown that locking effects (and results) are identical to the RM case, since no additional constraints arise as $d \to 0$.

3. *Locking in other error measures*: Locking is very dependent on the error measure under consideration. If, for instance, we take the moments M_x, M_y, M_{xy} at a point, then the locking effects are similar to those for the energy norm. See Fig. 18, where the moment M_x at the point (0.3, 0.8) is considered. If, on the other hand, we consider the shear stresses Q_x, Q_y, then the locking is significantly worse, since these involve an extra power d^{-1}. It is seen from Fig. 19 that little convergence is obtained for the h version, though the p version is still robust.

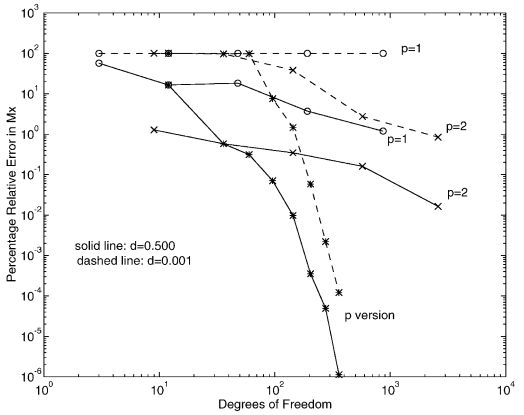

Fig. 18. Locking for the moment M_x at (0.3, 0.8).

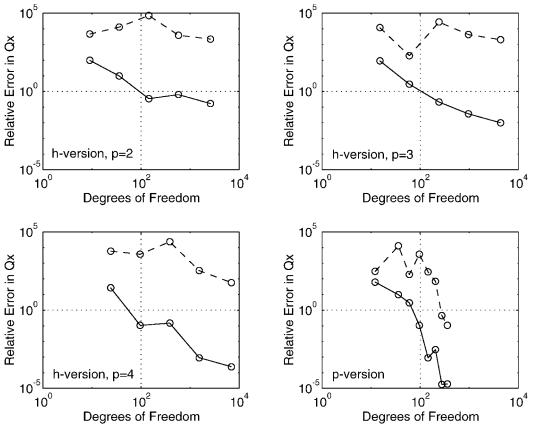

Fig. 19. Locking for the shear stress Q_x. Solid line: $d = 0.5$. Dashed line: $d = 0.001$.

4. *Mixed/reduced constraint methods*: For standard FEMs, the Kirchhoff constraint (6.1) must be satisfied *exactly* in the limit as $d \to 0$. In reduced constraint methods, we replace this constraint by

$$R_N K U_N = R_N(\nabla w_N + \boldsymbol{\phi}_N) = 0 \tag{6.7}$$

by defining a new bilinear form

$$B_N(U, V) = a(\boldsymbol{\phi}, \boldsymbol{\theta}) + \gamma\mu d^{-2}(R_N K U, R_N K V)$$

and solving problem (3.7) with B_N instead of B. Here, R_N is a projection into a suitable space of polynomials, that is generally defined piecewise over each element, and which is designed so that (6.7) is easier to satisfy than (6.1). Various choices of projections are discussed, e.g., in [30]. The analysis of such methods can then proceed either by analyzing separately an *approximation* and a *consistency* error [30], or by re-writing the method as a mixed method with the shear stress

$$\boldsymbol{q}_d = d^{-2}(\nabla w_d + \boldsymbol{\phi}_d)$$

as a new unknown (see, e.g., [36]).

In [36], we have analyzed an hp method based on the MITC reduction operators R_N [12]. This method has the advantage of being locking free both in h and in p. Moreover, uniform estimates in the shear stress can now be obtained. Some computational results using these elements may be found in [14].

5. *Some remarks on shells*: Locking effects in shells can be more serious than those in plates. In addition to shear locking, we may also observe *membrane* locking, which is a harder phenomenon to deal with. Moreover, there is strong interaction between locking and boundary layers. We refer to [28,23,18,38] where some hp methods (both standard and mixed) have been discussed to overcome these effects.

References

[1] D.N. Arnold, R. Falk, Asymptotic analysis of the boundary layer for the Reissner-Mindlin plate model, SIAM J. Math. Anal. 27 (1996) 486–514.

[2] I. Babuška, M.R. Dorr, Error estimates for the combined h and p version of the finite element method, Numer. Math. 37 (1981) 252–277.

[3] I. Babuška, B. Guo, Approximation properties of the h–p version of the finite element method, Comput. Methods Appl. Mech. Eng. 133 (1996) 319–346.

[4] I. Babuška, R.B. Kellogg, J. Pitkaranta, Direct and inverse estimates for finite elements with mesh refinement, Numer. Math. 33 (1979) 447–471.

[5] I. Babuška, L. Li, The h–p version of the finite element method in the plate modeling problem, Comm. Appl. Numer. Methods 8 (1992) 17–26.

[6] I. Babuška, L. Li, The problem of plate modeling, theoretical and computational results, Comput. Math. Appl. Mech. Eng. 100 (1992) 249–273.

[7] I. Babuška, M. Suri, The h–p version of the finite element method with quasiuniform meshes, RAIRO, Math. Mod. Numer. Anal. 21 (1987) 199–238.

[8] I. Babuška, M. Suri, On locking and robustness in the finite element method, SIAM J. Numer. Anal. 29 (1992) 1261–1293.

[9] I. Babuška, M. Suri, The p and hp versions of the finite element method, basic principles and properties, SIAM Rev. 36 (1994) 578–632.

[10] I. Babuška, B.A. Szabo, R. Actis, Hierarchic models for laminated composites, Internat. J. Numer. Methods Eng. 33 (1992) 503–535.

[11] I. Babuška, B.A. Szabo, I.N. Katz, The p-version of the finite element method, SIAM J. Numer. Anal. 18 (1981) 515–545.

[12] F. Brezzi, M. Fortin, R. Stenberg, Error analysis of mixed-interpolated elements for Reissner-Mindlin plates, Math. Models Methods Appl. Sci. 1 (1991) 125–151.

[13] P.G. Ciarlet, The Finite Element Method for Elliptic Problems, North-Holland, Amsterdam, 1978.

[14] L.D. Croce, T. Scapolla, Some applications of hierarchic high-order MITC finite elements for Reissner-Mindlin plates, in: P. Neittaanmaki, M. Krizek, R. Stenberg (Eds.), Finite Element Methods. Fifty Years of the Courant Element, Marcel Dekker, New York, 1994, pp. 183–190.

[15] M. Dauge, in: Elliptic Boundary Value Problems on Corner Domains, Lecture Notes in Mathematics, Vol. 1341, Springer, New York, 1988.

[16] M. Dauge, I. Gruais, Asymptotics of arbitrary order for a thin elastic clamped plate, Asymptotic Anal. Part I: 13 (1996) 167–197, Part II: 16 (1998) 99–124.

[17] M. Dauge, Z. Yosibash, Boundary layer realization in thin elastic 3-d domains and 2-d hierarchic plate models, Internat. J. Solids Struct. 37 (2000) 2443–2471.

[18] K. Gerdes, A. Matache, C. Schwab, Analysis of membrane locking in hp FEM for a cylindrical shell, Z. Angew. Math. Mech. 78 (1998) 663–686.

[19] P. Grisvard, Elliptic Problems in Non-smooth Domains, Pitman, Boston, 1985.

[20] W. Gui, I. Babuška, The h, p and h–p versions of the finite element method in one dimension (Parts 1–3), Numer. Math. 40 (1986) 577–683.
[21] B. Guo, I. Babuška, The h–p version of the finite element method I and II, Comput. Mech. 1 (1986) 21–41 and 203–226.
[22] H. Hakula, Licentiate Thesis, Helsinki University of Technology, 1997.
[23] H. Hakula, Y. Leino, J. Pitkaranta, Scale resolution, locking, and high-order finite element modeling of shells, Comput. Methods Appl. Mech. Eng. 133 (1996) 157–182.
[24] H. Han, R.B. Kellogg, Differentiability properties of solutions of the equation $-\varepsilon^2\Delta u + ru = f(x, y)$ in a square, SIAM J. Math. Anal. 21 (1990) 394–408.
[25] R.B. Kellogg, Boundary layers and corner singularities for a self-adjoint problem, in: M. Costabel, M. Dauge, S. Nicaise (Eds.), Lecture Notes in Pure and Applied Mathematics, Vol. 167, Marcel Dekker, New York, 1995, pp. 121–149.
[26] V.A. Kondrat'ev, Boundary value problems for elliptic equations in domains with conic or corner points, Trans. Moscow Math. Soc. 16 (1967) 227–313.
[27] J.M. Melenk, C. Schwab, hp FEM for reaction-diffusion equations I: robust exponential convergence, SIAM J. Numer. Anal. 35 (1998) 1520–1557.
[28] J. Pitkaranta, The problem of membrane locking in finite element analysis of cylindrical shells, Numer. Math. 61 (1992) 523–542.
[29] J. Pitkaranta, Y. Leino, O. Ovaskainen, J. Piila, Shell deformation states and the finite element method: A benchmark study of cylindrical shells, Comput. Methods Appl. Mech. Eng. 128 (1995) 81–121.
[30] J. Pitkaranta, M. Suri, Design principles and error analysis for reduced-shear plate-bending finite elements, Numer. Math. 75 (1996) 223–266.
[31] C. Schwab, p- and hp- Finite Element Methods, Oxford Science Publications, Oxford, 1998.
[32] C. Schwab, M. Suri, Locking and boundary layer effects in the finite element approximation of the Reissner–Mindlin plate model, Proc. Sympos. Appl. Math. 48 (1994) 367–371.
[33] C. Schwab, M. Suri, The p and hp version of the finite element method for problems with boundary layers, Math. Comp. 65 (1996) 1403–1429.
[34] C. Schwab, M. Suri, C. Xenophontos, The hp finite element method for problems in mechanics with boundary layers, Comput. Methods Appl. Mech. Eng. 157 (1998) 311–333.
[35] G.I. Shishkin, Grid approximation of singularly perturbed parabolic equations with internal layers, Soviet J. Numer. Anal. Math. Modelling 3 (1988) 393–407.
[36] R. Stenberg, M. Suri, An hp error analysis of MITC plate elements, SIAM J. Numer. Anal. 34 (1997) 544–568.
[37] M. Suri, Analytical and computational assessment of locking in the hp finite element method, Comput. Methods Appl. Mech. Eng. 133 (1996) 347–371.
[38] M. Suri, A reduced constraint hp finite element method for shell problems, Math. Comp. 66 (1997) 15–29.
[39] M. Suri, I. Babuška, C. Schwab, Locking effects in the finite element approximation of plate models, Math. Comp. 64 (1995) 461–482.
[40] B.A. Szabo, I. Babuška, Finite Element Analysis, Wiley, New York, 1991.
[41] B.A. Szabo, A.K. Mehta, p-convergent finite element approximations in fracture mechanics, Internat. J. Numer. Methods Eng. 12 (1978) 551–560.
[42] M.J. Turner, R.W. Clough, H.C. Martin, L.J. Topp, Stiffness and deflection analysis of complex structures, J. Aeronaut. Sci. 23 (1956) 805–823.
[43] R. Vulanović, D. Herceg, N. Petrović, On the extrapolation for a singularly perturbed boundary value problem, Computing 36 (1986) 69–79.
[44] C. Xenophontos, The hp version of the finite element method for singularly perturbed boundary value problems, Doctoral Dissertation, University of Maryland, Baltimore County, May 1996.
[45] C. Xenophontos, The hp finite element method for singularly perturbed problems in smooth domains, Math. Models Methods Appl. Sci. 8 (1998) 299–326.
[46] C. Xenophontos, Finite element computations for the Reissner–Mindlin plate model, Comm. Numer. Methods Eng. 14 (1998) 1119–1131.
[47] C. Xenophontos, The hp finite element method for singularly perturbed problems in nonsmooth domains, Numer. Methods PDEs 27 (1999) 63–89.